2011 American Control Conference
on O'Farrell Street, San Francisco, CA, USA
June 29 - July 01, 2011

Optimal Sensor Placement for Health Monitoring of Civil Structures

Gwendolyn W. van der Linden**, Abbas Emami-Naeini*,
Robert L. Kosut*, Hassan Sedarat*, and Jerome P. Lynch‡

Abstract— **In this paper we focus on comparing three candidate approaches to the optimal placement of sensors for state estimation-based continuous health monitoring of structures. The first aims to minimize the static estimation error of the structure deflections, using the linear stiffness matrix derived from a finite element model. The second approach aims to maximize the observability of the derived linear state space model. The third approach aims to minimize the dynamic estimation error of the deflections using a Linear Quadratic Estimator. Both nonlinear mixed-integer and relaxed convex optimization formulations are presented. A simple search-based optimization implementation for each of the three approaches is demonstrated on a model of the long-span New Carquinez Bridge in California.**

I. Introduction

The deterioration of our national infrastructure is driving the need for objective information associated with infrastructure health management, and has motivated infrastructure owners to begin adopting continuous and autonomous monitoring of their assets through the use of permanent monitoring systems [1]. These structural health monitoring (SHM) systems are designed to generate quantitative measurements that empower objective and cost-effective evaluation of bridge conditions. Ultimately, a structural health monitoring system needs to address the following question unequivocally:

”Is the structure OK?”

The answer needs to be expressed in terms of simple actionable choices, e.g., using three levels (1) Green (OK), (2) Yellow (Warning: inspect specific places on the structure for corrective maintenance), or (3) Red (Shutdown/evacuate the structure immediately).

For predictive maintenance (yellow flag), as contrasted with scheduled maintenance, the goal is to use sensor readings together with mathematical models of the bridge to predict the health of the bridge and generate real-time actionable maintenance protocols. It can be expected that only doing required inspection (in a predictive fashion) will be much less expensive than performing scheduled, and often unnecessary, inspection. This approach will involve the use of sensing (for stress, deformation, corrosion, etc.), wireless communication, advanced structural modeling, system identification, grid computing, embedded software, decision science, and other relevant tools. More specifically, the system will require the efficient integration of sensor technology, optimal sensor placement, wireless sensor networking, structural system identification, distributed simulation, and data management within a network. For bridge health monitoring a typical flow of information and data sizes for estimation are shown in Fig. 1. A high-fidelity physics-based model of the bridge is developed using finite elements, based on the as-built drawings. The bridge model is used for a number of purposes: (a) to compute the optimal sensor placement, which is used when instrumenting the bridge, (b) to generate the reduced order pseudo-inverse model (estimator) to estimate loads (unknown inputs), (c) in the full-order feed-forward model to estimate the strains at modeled elements, and finally (d) in load capacity and fatigue models to estimate the current health of the bridge.

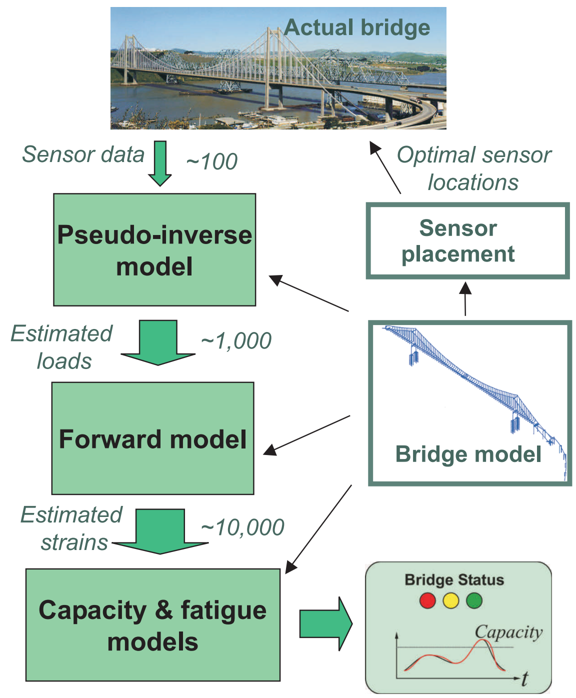

Fig. 1. Flow of information & typical number of variables for bridge health monitoring.

An important task in implementing a structural health monitoring system is determining the optimal *number* and *locations* of the sensors. There is extensive literature on optimal sensor placement (OSP) in aerospace structures [2], process control industry [3], [4], nuclear power plants [5], and bridges [6], [7]. The studies range from heuristic approaches

*van der Linden, Emami-Naeini, Kosut, and Sedarat are with SC Solutions, Inc., 1261 Oakmead Pkwy, Sunnyvale, CA 94085, USA.

‡Lynch is with the Department of Civil and Environmental Engineering & Department of Electrical Engineering and Computer Science, University of Michigan, 2380 G.G. Brown Laboratory, Ann Arbor, MI 48109-2125, USA.

*For correspondence contact van der Linden: glinden@scsolutions.com.

978-1-4577-0079-8/11/$26.00 ©2011 AACC

based on engineering judgment to systematic optimization approaches based on mathematical system models. There are two distinct aspects of health monitoring that influence OSP: detecting damage as early as possible, and determining fatigue levels even before damage occurs. The first approach can be posed as *model identification*: to detect changes in behavior of the structure as an indicator of damage. The latter approach can be posed as *state estimation*: by estimating the state of the structure (i.e. the displacements in case of a static system, and displacements and velocities in case of a dynamic system), it is possible to estimate the stresses and strains of the structure over time, or compute the accumulated fatigue. The majority of publications on OSP for SHM focus on the model identification approach.

In this paper we focus on OSP for state estimation-based continuous SHM of structures using three approaches, of increasing computational complexity. The first method aims to minimize the static estimation error of the structure deflections, using the linear stiffness matrix derived from a finite element (FE) model. The second approach aims to maximize the observability Gramian of the derived linear state space model. The third approach aims directly at minimizing the dynamic estimation error of the deflections using a Linear Quadratic Estimator (LQE). Each method is evaluated using a finite element model of the long-span New Carquinez Bridge in California.

The paper is organized as follows. In Section II a generic bridge model is introduced. Each of the OSP approaches (static estimation, observability and dynamic estimation) is defined in Sections III, IV and V respectively. Finally, the results are presented in Section VI and the conclusions appear in Section VII.

II. Bridge model

The OSP methods described in this paper are applied to a model of the New Carquinez Bridge, which is a long span suspension bridge, managed by Caltrans (California DOT). The bridge connects the Solano and Contra Costa Counties, is located between Vallejo (on the North side) and Crockett (on the South side) in California, and has a length of 1056 m (3465 ft), with a main span of 728 m (2389 ft).

A simplified 2D finite element model of the bridge has been created that includes the anchors, towers, and deck, with a total of 270 nodes. Figure 2 shows the 2D model, with the heavy dots indicating a potential sensor selection. It is assumed that there are 80 potential sensor locations, all on the roadbed nodes of the bridge.

For the examples below the model inputs and outputs are limited to the vertical motion of the bridge deck. For the loads considered here, the bridge operates within the linear regime. Based on the finite element model locally linear static and dynamic models are constructed.

A. Static linear model

Assuming the dynamics are sufficiently fast, the structure can be approximated by:

$$\delta = Gf,\ G \in \mathbf{R}^{n\times p} \tag{1}$$

where G is the flexibility matrix, δ the deflection, and f the vertical forces on the roadbed. The forces f are assumed to be independent random variables:

$$f \in \mathcal{N}(0, V_f). \tag{2}$$

We assume that we can measure any of the roadbed deflections:

$$y = C_s\delta + w,\ w \in \mathcal{N}(0, V_w) \tag{3}$$

where w is the measurement noise, C_s is the sensor output matrix and y is the measured output.

B. Dynamic linear model

Assuming the dynamics are relevant, the structure can be approximated by:

$$\begin{aligned} &\mathcal{M}\ddot{\delta} + \mathcal{C}\dot{\delta} + \mathcal{K}\delta = \mathcal{H}f, \\ &\mathcal{M}, \mathcal{C}, \mathcal{K} \in \mathbf{R}^{n\times n},\ \mathcal{H} \in \mathbf{R}^{n\times p}, \end{aligned} \tag{4}$$

where $\mathcal{M}$ is the mass matrix, $\mathcal{C}$ the damping matrix, $\mathcal{K}$ the stiffness matrix, δ the deflection, $\mathcal{H}$ the input matrix, and f the vertical forces exerted on the roadbed. We assume that we can potentially measure any of the roadbed deflections. Equation (4) can be rewritten in standard state-space form:

$$\left\{ \begin{array}{lcl} \dot{x} &=& Ax + Bf \\ \delta &=& C_\delta x \\ y &=& C_d x + w \end{array} \right. \tag{5}$$

where:

$$x = \begin{bmatrix} \delta \\ \dot{\delta} \end{bmatrix} \tag{6}$$

$$A = \begin{bmatrix} 0 & I \\ -\mathcal{M}^{-1}\mathcal{K} & -\mathcal{M}^{-1}\mathcal{C} \end{bmatrix} \tag{7}$$

$$B = \mathcal{M}^{-1}\mathcal{H} \tag{8}$$

$$C_\delta = \begin{bmatrix} I & 0 \end{bmatrix} \tag{9}$$

$$C_d = \begin{bmatrix} C_s & 0 \end{bmatrix} \tag{10}$$

$$f \in \mathcal{N}(0, V_f) \tag{11}$$

$$w \in \mathcal{N}(0, V_w) \tag{12}$$

and w is measurement noise, x is the state vector, and y is the measured output vector.

III. Static estimation

Using the static linear model (see Section II-A), the maximum *a posteriori* (MAP) estimate [8] of f from measured data y, see (3), gives:

$$\hat{f} = \left(V_f^{-1} + G^T C_s^T V_w^{-1} C_s G\right)^{-1} G^T C_s^T V_w^{-1} y, \tag{13}$$

with the associated covariance matrix:

$$\operatorname{cov}\ \hat{f} = \left(V_f^{-1} + G^T C_s^T V_w^{-1} C_s G\right)^{-1}. \tag{14}$$

With $\hat{x} = G\hat{f}$, then the covariance matrix of the state estimate is:

$$\begin{aligned} &\operatorname{cov}\ \hat{x} = G\ (\operatorname{cov}\ \hat{f})\ G^T = \\ &G\left(V_f^{-1} + G^T C_s^T V_w^{-1} C_s G\right)^{-1} G^T. \end{aligned} \tag{15}$$

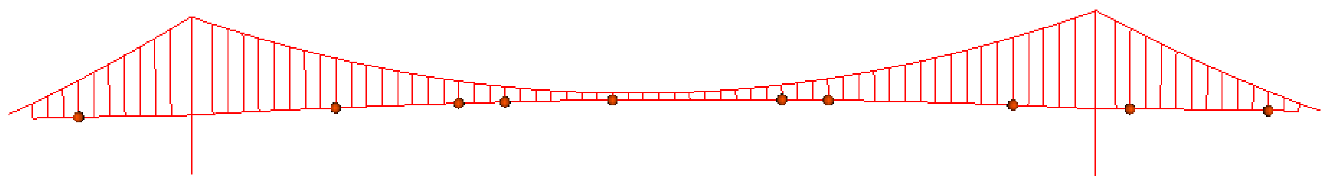

Fig. 2. A schematic of the New Carquinez Bridge 2D model with potential sensor locations.

Introducing θ as the vector of sensor selections, where a value of 1 means that the corresponding output is selected for sensing, and 0 means that it is not selected, the static estimation-based optimal sensor selection problem can be posed as the standard optimization problem:

$$\begin{aligned} &\min_{\theta} \phi(\text{cov } \hat{x}(\theta)) \\ &\text{s.t. } \begin{cases} \theta_i \in \{0,1\} \\ \mathbf{1}^T\theta = m \end{cases} \end{aligned} \tag{16}$$

where m is the number of sensors, $\mathbf{1}$ is a vector of ones and $\phi(X)$ is a measure of the covariance size, such as $\text{Tr}(X)$, $||X||$ or $\log\det(X)$, and $C_{s,i}$ is defined as the i'th row of C_s:

$$\begin{aligned} &\text{cov } \hat{x}(\theta) = G\left(V_f^{-1} + G^T H_s(\theta) G\right)^{-1} G^T, \\ &H_s(\theta) = \textstyle\sum_{i=1}^m \theta_i C_{s,i}^T V_w^{-1} C_{s,i}, \end{aligned} \tag{17}$$

which is a mixed-integer optimization problem.

A. Solving the mixed-integer optimization problem

The optimization problem described by (16) requires an exhaustive search to find the global optimum, but a local optimum can be found using a simple search algorithm:

1) **Initialize.** Start with an empty set of selected sensors.
2) **Add most relevant sensor.** Test adding each unselected sensor to the set of selected sensors, one at a time, and keep the one giving the lowest cost function value.
3) **Remove redundant sensor, if any.** Test removing each of the selected sensors, one at a time, and remove the least important one if the resulting set hasn't been selected before.
4) Go back to step 2 until the maximum number of sensors is reached, or a sufficiently low cost function value is achieved.

This approach is applied to the static simplified model, and can also be applied to the next two approaches (see Sections IV and V). Note that the maximum number of sensors m can be set to the maximum number of sensors that can be reasonably afforded. Also note that if certain locations are unsuitable for placing sensors, they can simply be removed from the set of potential sensor locations. Some locations may be unsuitable for placing sensors due to the harsh environment, inaccessibility, etc. The optimization results may provide further guidance in reducing the number of sensors by evaluating the achieved cost function value as a function of the number of sensors.

B. Solving the relaxed convex optimization problem

Approximate solutions to (16) can be obtained via *relaxation* to a convex optimization problem [9]. Convex optimization problems are readily solved using available software and computational methods [10]. Equation (16) can be converted to a relaxed sensor selection problem as the following standard optimization problem:

$$\begin{aligned} &\min_{\theta} \phi(\text{cov } \hat{x}(\theta)) \\ &\text{s.t. } 0 \le \theta_i \le 1, \;\; \mathbf{1}^T\theta = m. \end{aligned} \tag{18}$$

Choosing $\phi(X) = \text{Tr}(X)$, (18) can be converted to the *convex* optimization problem:

$$\begin{aligned} &\min_{Q,\theta} \text{Tr}(Q) \\ &\text{s.t. } \begin{cases} \begin{bmatrix} Q & G \\ G^T & V_f^{-1} + G^T H_s(\theta) G \end{bmatrix} \ge 0 \\ 0 \le \theta_i \le 1, \\ \mathbf{1}^T\theta = m. \end{cases} \end{aligned} \tag{19}$$

The constraint $\theta_i \in \{0,1\}$ is relaxed to allow θ_i to take any value between 0 and 1. Once the optimum is found, an approximate solution must be generated by rounding the values to either 0 or 1, see [9]. The resulting optimal value of ϕ is a *lower bound* on the mixed integer problem in (16). In principle, the above optimization problem can be solved using standard convex optimization tools. However, even for small finite element models the resulting problem size requires special handling, which is still under development. For now, we refer to the approach in Section III-A as an *upper bound* on the solution that can be achieved with the convex optimization approach.

IV. Observability Gramian

In the case of dynamic estimation, the goal is to estimate the deflections from the selected sensor measurements. An important system property in this context is the observability of the system state [11], which indicates to what extend the state can be reconstructed from the output signal. We solve the optimization problem:

$$\begin{aligned} &\min_{\theta} \text{Tr}(P^{-1}) \\ &\text{s.t. } \begin{cases} A^T P + PA + \sum_i \theta_i C_{d,i}^T C_{d,i} = 0, \\ P^T = P \ge 0, \end{cases} \end{aligned} \tag{20}$$

where P is the observability Gramian matrix (for a stable system). This problem can be solved using the search method discussed in Section III-A.

Note that the above optimization problem is not linear or quadratic in the parameters (P and θ_i), and as a consequence cannot be readily solved using convex optimization tools. By introducing Q such that:

$$P^{-1} \leq Q \quad \Leftrightarrow \tag{21}$$

$$\begin{bmatrix} Q & I \\ I & P \end{bmatrix} \geq 0 \tag{22}$$

the problem can be rewritten as the equivalent convex optimization in P, Q and θ, formulated as:

$$\begin{aligned} &\min_{\theta} \mathrm{Tr}(Q) \\ &\text{s.t.} \begin{cases} A^T P + PA + \sum_i \theta_i C_{d,i}^T C_{d,i} = 0, \\ P \geq 0, \\ \begin{bmatrix} Q & I \\ I & P \end{bmatrix} \geq 0, \\ 0 \leq \theta_i \leq 1, \\ \mathbf{1}^T \theta = m. \end{cases} \end{aligned} \tag{23}$$

V. DYNAMIC ESTIMATION

As an alternative to observability, the sensor selection problem can be directly posed as finding the set of sensors that yields the best dynamic estimator performance. Using the linear dynamic model in (5) we can construct a Linear Quadratic Estimator (LQE):

$$\dot{\hat{x}} \;=\; (A - LC_d)\hat{x} + Ly \tag{24}$$

$$\hat{\delta} \;=\; C_\delta \hat{x} \tag{25}$$

where:

$$\begin{aligned} 0 &= AP + PA^T - PH_d(\theta)P + BV_f B^T, \\ H_d(\theta) &= \textstyle\sum_{i=1}^m \theta_i C_{d,i}^T V_w^{-1} C_{d,i}, \\ L &= P\left(\textstyle\sum_i \theta_i C_d\right)^T V_w^{-1}. \end{aligned} \tag{26}$$

P, the solution to the Algebraic Riccati Equation (26), is equal to the covariance of the state estimation error, so

$$cov(\delta - \hat{\delta}) \;= C_\delta P C_\delta^T. \tag{27}$$

As a result, the dynamic estimation-based sensor placement problem can be posed as:

$$\begin{aligned} &\min_{\theta} \phi(C_\delta P C_\delta^T) \\ &\text{s.t.} \\ &\begin{cases} AP + PA^T - PH_d(\theta)P + BV_f B^T = 0 \\ \theta_i \in \{0, 1\} \\ \mathbf{1}^T \theta = m. \end{cases} \end{aligned} \tag{28}$$

Note that (26) is not linear or quadratic in the parameters (P and θ_i). By introducing:

$$S \;=\; P^{-1} \tag{29}$$

(26) can be converted to an equivalent Algebraic Riccati Equation (ARE):

$$0 = A^T S + SA - H_d(\theta) + SBV_f B^T S, \tag{30}$$

which is quadratic in the parameters. This in turn can be rewritten as a Linear Matrix Inequality (LMI) [12], which is linear in the parameters (S and θ_i):

$$\begin{aligned} \begin{bmatrix} A^T S + SA - H_d(\theta) & SB \\ B^T S & -V_f^{-1} \end{bmatrix} &\geq 0, \\ S &\geq 0. \end{aligned} \tag{31}$$

The sensor placement can be formulated as minimization of the estimation error covariance matrix defined in (27), leading to the following optimization problem:

$$\begin{aligned} &\min_{S,\theta} \mathrm{Tr}(C_\delta S^{-1} C_\delta^T) \\ &\text{s.t.} \begin{cases} \begin{bmatrix} A^T S + SA - H_d(\theta) & SB \\ B^T S & -V_f^{-1}, \end{bmatrix} \geq 0, \\ S \geq 0. \end{cases} \end{aligned} \tag{32}$$

This can be rewritten as the convex optimization problem in the variables S, Q and θ:

$$\begin{aligned} &\min_{S,Q,\theta} \mathrm{Tr}(Q) \\ &\text{s.t.} \begin{cases} \begin{bmatrix} A^T S + SA - H_d(\theta) & SB \\ B^T S & -V_f^{-1} \end{bmatrix} \geq 0, \\ \begin{bmatrix} Q & C_\delta \\ C_\delta^T & S \end{bmatrix} \geq 0, \\ 0 \leq \theta_i \leq 1, \\ \mathbf{1}^T \theta = m. \end{cases} \end{aligned} \tag{33}$$

VI. RESULTS

The sensor selections have been determined for the simplified 2D model of the New Carquinez Bridge discussed in Section II. For each sensor placement approach the results are shown in a plot with two subplots. In the top sub-plot (cost function value graph, or *cost graph*, not to be confused with monetary cost) shows the cost function value (vertical axis) as a function of the number of selected sensors (horizontal axis). The bottom sub-plot (sensor location graph) is a schematic depiction of the location of the selected sensors (horizontal axis) as a function of the number of selected sensors (vertical axis). For a given number of sensors, the dots on the corresponding (imaginary) horizontal line show location of the sensors. By definition the number of dots (sensors) on a horizontal line equals the sensor count value.

Note that in all three methods the cost function is some direct or indirect measure of the estimation error. Therefore, the cost graph is very helpful in selecting the number of sensors to use, as it shows how much the cost function value is decreased by adding another sensor (moving to the right in the top sub-plot), while the sensor location graph shows which sensors are added or moved as more sensors are used (moving up in the bottom sub-plot). Note that the cost for each OSP approach is defined differently, and should not be compared between figures. In all plots the case of 12 selected sensors is highlighted.

Figure 3 shows the results for the static estimation-based OSP problem (16), Figure 4 shows the results for the observability-based OSP problem (20), and Figure 5 shows the results for the static estimation-based OSP problem

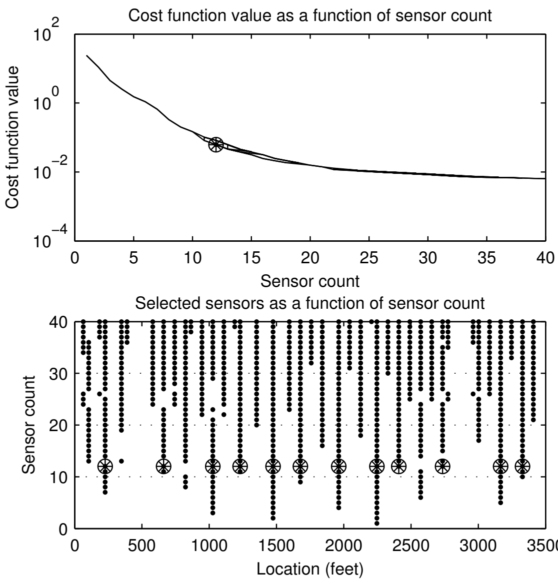

Fig. 3. Sensor selection result from the static estimation method.

(28). Each of the figures show a similar pattern: all three methods show a significant decline in cost function value when selecting from 1 up to 20 sensors, and they all show sensor locations that are spread out along the length of the bridge, although not uniformly.

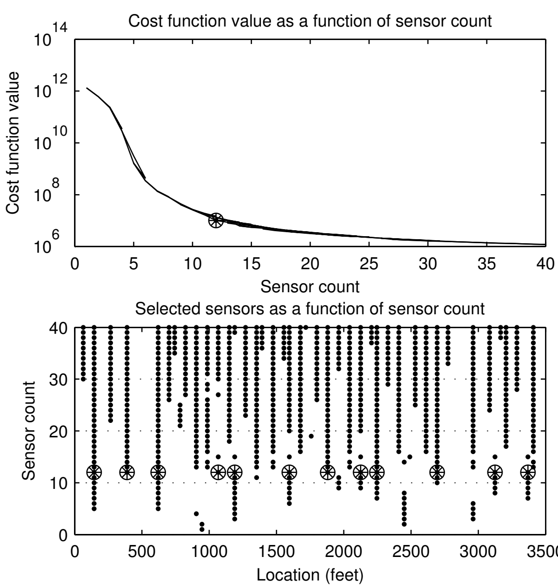

Fig. 4. Sensor selection result from the observability method.

Note that the static estimation OSP problem in (16) involves an $n \times n$ matrix inverse, which is implemented efficiently using Gaussian elimination. The observability OSP problem in (20) involves solving a $2n \times 2n$ Lyaponuv equation. Finally, the dynamic estimation OSP problem in (28) involves solving a $2n \times 2n$ Algebraic Riccati Equation. The time to compute each of the cases on an Intel-based computer (Intel Core Duo, 2.16GHz) is shown in Table I.

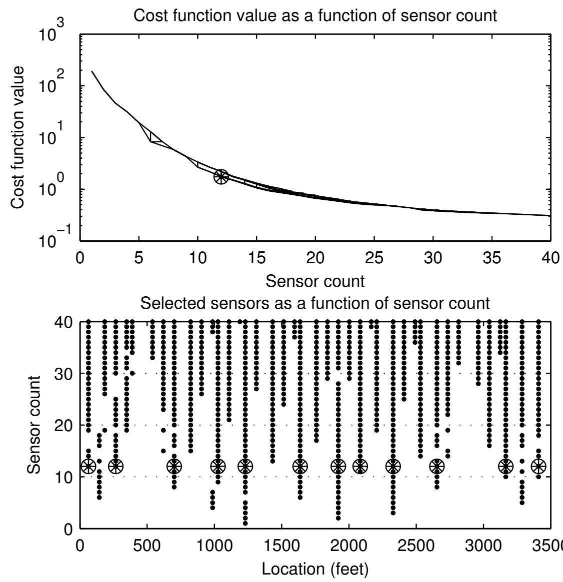

Fig. 5. Sensor selection result from the dynamic estimation method.

TABLE I

COMPUTATION TIME FOR 40 SENSORS.

Approach	Time (mm:ss)
Static estimation	00:32
Observability	09:45
Dynamic estimation	56:20

As expected the static estimation-based approach is the fastest. The observability-based approach is about 18 times slower, and the dynamic estimation-based approach another 6 times slower (more than 100 times slower than the first method).

VII. CONCLUSIONS

We have proposed and compared three approaches to the Optimal Sensor Placement (OSP) for estimation-based health monitoring of civil structures: based on minimizing the static displacement estimation error, minimizing the inverse of the observability, and minimizing the dynamic displacement estimation error respectively. Each of these approaches leads to a nonlinear mixed-integer optimization problem for which a locally optimal solution can be found using an iterative search algorithm. Each of these approaches can also be relaxed to a convex optimization problem, for which a global optimal solution can be found. However, the solution to the relaxed problem must be approximated to generate a discrete sensor selection. Specialized software is required to handle the convex optimization in case of the large model orders anticipated.

Each of the approaches is implemented and applied to a simple 2D model of the long-span New Carquinez Bridge in California. The dynamic estimation error as a function of sensor count shows a similar performance of all the methods, see Fig. 6. In addition, the resulting sensor placement solutions are similar for each of these approaches, but certainly

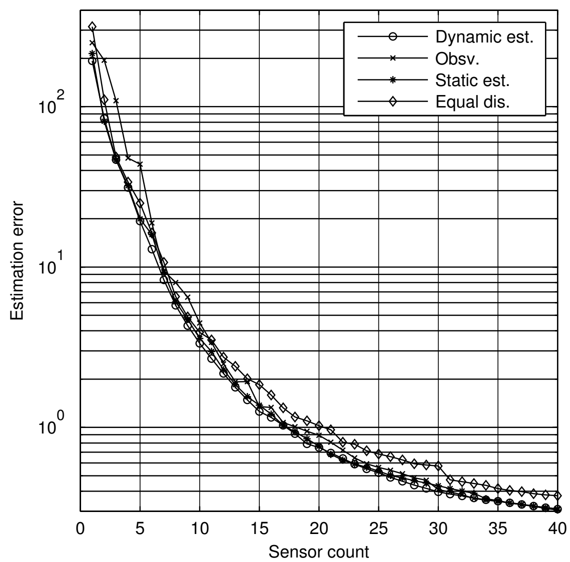

Fig. 6. Comparison of methods using dynamic estimation error.

not identical. While by far the most computationally intensive, the dynamic estimation-based OSP approach captures the actual sensor placement problem for state estimation-based health monitoring. Note that the results are based on a small model (270 nodes); structural health monitoring of large structures requires detailed finite element models that are significantly larger (>10,000 nodes), which significantly increases the required computation time. More study is needed to determine if, e.g., the more computationally efficient observability-based or static estimation OSP approaches yield sufficiently good results.

The next goal is to apply OSP to detailed 3D finite element-based bridge models, and, as a practical application, use the generated results for efficiently instrumenting the New Carquinez Bridge [13]. This involves implementing the optimization algorithms using specialized efficient convex solvers, and integrating model-reduction techniques into the approach. In order to assess fatigue, the most common method is the so-called "Rain Flow Counting" [14], [15] which requires strain estimates rather than deflection. Estimating strain may very well place sensors at entirely different locations than those shown here for deflection.

If the methods can solve OSP of the larger models in reasonable time, they can be extended to include additional requirements, such as robustness to sensor failure: place n sensors such that the worst case cost function value of the cases with up to m sensor failures is minimized, leading to a min-max optimization problem.

We plan to integrate the most suitable OSP method into a software tool that can generate an optimized sensor placement plan based on a detailed finite element model, and plan to publish on these efforts in the future.

VIII. ACKNOWLEDGMENTS

The work presented here is sponsored by NIST as part of the NIST TIP 2008 program: *Cyber-Enabled Wireless Monitoring Systems for the Protection of Deteriorating National Infrastructure Systems*. We also want to thank Caltrans (California Department of Transportation) for their generous support. We are grateful to the anonymous reviewers for their constructive feedback.

REFERENCES

[1] J. P. Lynch, V. Kamat, V. C. Li, M. Flynn, D. Sylvester, K. Najafi, T. Gordon, M. Lepech, A. Emami-Naeini, A. Krimotat, M. Ettouney, S. Alampalli, and T. Ozdemir, "Overview of a cyber-enabled wireless monitoring system for the protection and management of critical infrastructure systems," in *Proceedings of the SPIE Conference on Smart Structures and Materials, San Diego, CA*, 2009.

[2] S. L. Padula, D. L. Palumbo, R. K. Kincaid, S. L. Padula, D. L. Palumbo, and R. K. Kincaid, "Optimal sensor/actuator locations for active structural acoustic control," in *Proceedings of the 39th AIAA/ASME/ ASCE/AHS/ASC Structures, Dynamics and Materials Conference*, no. 98–1865. TSYNKOV, 1998.

[3] D. M. Naimimohasses, D. M. Barnett, and P. R. Smith, "Sensor optimization using neural network sensitivity measures," *Measurement Science Technology*, no. 6, pp. 1291–1300, 1995.

[4] R. L. Kosut and M. G. Kabuli, "On actuator-sensor selection in thermal processes," in *Proceedings of the 34th Conference on Decision & Control*, December 1995, pp. 2482–2483.

[5] D. Y. Oh and H. C. No, "Determination of the minimal number and optimal sensor location in a nuclear system with fixed incore detectors," *Nuclear Engineering and Design*, no. 152, pp. 197–212, 1994.

[6] M. Meo and G. Zumpano, "On the optimal placement techniques for a bridge structure," *Engineering Structures*, vol. 27, pp. 1488–1497, 2005.

[7] J. M. Beal, A. Shukla, O. A. Brezhneva, and M. A. Abramson, "Optimal sensor placement for enhancing sensitivity to change in stiffness for structural health monitoring," *Optimization and Engineering*, vol. 9, no. 2, pp. 119–142, 2008.

[8] L. Ljung, *System Identification: Theory for the User (2nd Edition)*. Prentice Hall PTR, December 1998.

[9] S. Joshi and S. Boyd, "Sensor selection via convex optimization," *IEEE Transactions on Signal Processing*, vol. 57, no. 2, pp. 451–462, 2009.

[10] S. Boyd and L. Vandenberghe, *Convex Optimization*. Cambridge University Press, March 2004.

[11] G. F. Franklin, J. D. Powell, and A. Emami-Naeini, *Feedback Control of Dynamic Systems, 6th edition*. Prentice-Hall, 2010.

[12] S. Boyd, L. El Ghaoul, E. Feron, and V. Balakrishnan, *Linear Matrix Inequalities in System and Control Theory*, ser. Studies in Applied Mathematics. Society for Industrial Mathematics (SIAM), 1994, vol. 15.

[13] M. Kurata, J. P. Lynch, G. W. van der Linden, V. Jacob, and P. Hipley, "Preliminary study of a wireless structural monitoring system for the new carquinez suspension bridge," in *Proceedings of the Fifth World Conference on Structural Control and Monitoring*, 2010.

[14] M. Matsuiski and T. Endo, "Fatigue of metals subjected to varying stress," *Japan Soc. Mech. Engineering*, 1969.

[15] S. D. Downing and D. F. Socie, "Simple rainflow counting algorithms," *International Journal of Fatigue*, vol. 4, no. 1, pp. 31–40, January 1982.